Adsorption of DNA into Mesoporous Silica

Sean M. Solberg and Christopher C. Landry*

Department of Chemistry, University of Vermont, 82 University Place, Burlington, Vermont 05405

Received: March 17, 2006; In Final Form: June 1, 2006

In these experiments, double-stranded, linear DNA sequences were adsorbed into the pores of spherically shaped acid-prepared mesoporous silica (APMS). The lengths of the sequences were either 760 base pairs or 2000 base pairs. DNA adsorption into the interior of the mesoporous material was confirmed using confocal microscopy of sequences containing fluorescently labeled DNA molecules. Additional characterization with N_2 physisorption and powder X-ray diffraction supported this finding. The extent of adsorption was measured at various concentrations using UV−visible spectrophotometry to establish adsorption isotherms. APMS alone adsorbed a negligible amount of DNA; however, exchanging divalent cations such as Mg^{2+} and Ca^{2+} into the pores of APMS prior to DNA uptake was found to cause a significant amount of DNA to be adsorbed. Using Na^+ caused a lower amount of DNA to be adsorbed. DNA adsorption was also dependent on the pore diameter of APMS. Adsorption increased upon expansion of the pore size of the metal ion-exchanged material from 34 to 54 Å; however, no additional uptake was measured by further increasing the pore size to 100 Å. The amount of DNA adsorbed could also be significantly increased by using (aminopropyl)triethoxysilane to covalently link ammonium ions to the surface. Postsynthetic modification of the silica surface with aminopropyl groups increased the maximum DNA adsorption to 15.7 μg/mg silica, for materials with pore diameters of 100 Å, which is 2 to 3 times more adsorbed DNA than for metal ion-exchanged material. This indicated that DNA binds more strongly in the presence of the ammonium group compared to the metal counterions. Finally, calculation and comparison of Freundlich and Langmuir constants for these adsorption processes indicate that intermolecular interactions between the DNA molecules within the pores are significant when the effective pore diameter is small, including materials with larger pores that were modified with organosilane.

Introduction

The prospect of gene therapy and genetic engineering as a new medical technique has highlighted the challenges involved in transferring custom genetic material into cellular environments to correct genetic diseases. Currently, only a few methods are used to deliver and protect DNA during cellular transfection. The most common and simple method of gene delivery is the viral vector system, whereby a nonpathogenic virus is used as the method of transport. By manipulating the viral genome, viral genes can be modified with custom genetic material and grown in cell cultures to produce large quantities of viruses, which are then applied to cells for targeting various genetic diseases. Several classes of viral vectors have been developed such as retro-, adeno-, and adeno-associated viral vectors.[1] Clinical trials with viral vectors have shown that this method can be effective in DNA delivery and expression;[2] however, the procedure has been limited by the risks involved in expression of the viral genetic code, as well as its nonspecificity.[3] This has led to the engineering of many synthetic systems to package and deliver DNA to cells. Most synthetic delivery systems have been developed around a lipid/DNA or polymer/DNA scheme. Cationic liposome systems interact with negatively charged DNA to form complexes capable of entering the cell.[4] Of such conjugates, Lipofectamine is the most widely recognized liposome system. Similarly, ionic polymer systems have been extensively engineered into complexes for DNA delivery.[5,6] Among these include vectors based on cationic poly(ethyleneimine)[7] and poly(ethyleneoxide).[8] Although these systems have been extensively developed and studied, ineffective delivery and cytotoxicity issues remain prevalent. More recently, synthetic nanoparticles with cationic surfaces have provided an alternative approach to DNA delivery.[9] Amorphous silica nanoparticles are particularly attractive due to their high chemical resistance to microbial attack, low toxicity, thermal stability, and ease of modification.[10] Several attempts have been made to modify the external surface of silica nanoparticles materials for DNA binding by the attachment of cationic linkers that electrostatically bind DNA molecules.[11−13]

Mesoporous silica, formed by polymerizing a silica source in the presence of surfactants, has attracted tremendous research interest since it was first reported in 1992.[14] These materials typically possess large surface areas (in excess of 1000 m^2/g) and large internal pore volumes and have narrow pore size distributions that can be tailored during synthesis. These characteristics have led to the study of mesoporous silica materials in a range of applications where porosity is an important feature, such as catalysis and chromatography.[15,16] The large surface area and the controllable pore diameters have also made mesoporous silica attractive as a potential delivery agent for guest molecules, which can be easily adsorbed into their pores by ion exchange or covalent bonding for later release within cells.[17,18] Recent studies[19] have focused on the immobilization of metals,[20] proteins,[21−24] enzymes,[25−27] and drug molecules[28−30] into mesoporous silica. Increased uptake capacities (as compared to nonporous materials) have been observed, and subsequent studies involving release of the adsorbed

* To whom correspondence should be addressed. Fax: +1 802 656 0270. E-mail: christopher.landry@uvm.edu.

10.1021/jp061691+ CCC: $33.50
Published on Web 07/19/2006

molecules have laid the groundwork for the use of mesoporous materials as delivery agents.

In contrast to most forms of mesoporous silica, acid-prepared mesoporous silica (APMS) has a distinctive spherical shape that is particularly useful in applications involving microscopy and chromatography.[31] The synthesis of APMS is complete in less than 2 h, and the particle size and pore diameter of APMS are easily controlled simply by altering a set of standard reaction conditions. As with most forms of amorphous silica, its internal and external surfaces are easily functionalized through reaction with organosilanes. We have recently shown that APMS is an effective substrate for chromatography and catalysis;[32−37] however, its large surface area and tunable spherical particle size also make it an attractive candidate as a vector for cellular transfection. Prior to these studies, data must be gathered regarding the conditions required for effective adsorption and desorption of DNA within the pores. To date, there has been only one study describing the adsorption of DNA within mesoporous silica.[38] However, this study did not use APMS as the mesoporous substrate and was somewhat limited in the methods used to adsorb DNA. In this report, we describe the loading of APMS with linear double-stranded DNA. DNA adsorption is studied as a function of pore size and the type of organic functionality or inorganic ion used to bind the DNA. X-ray diffraction, nitrogen physisorption, UV−visible spectroscopy, and fluorescence confocal microscopy before and after pore filling are used to demonstrate that genetic material is taken up into the pores of APMS. We also attempt to define optimal conditions for DNA adsorption and quantify the maximum amount of DNA that can be adsorbed for a specific set of conditions.

Experimental Section

Materials and Methods. Powder X-ray diffraction (XRD) experiments were performed on a Scintag X1 $\theta-\theta$ diffractometer equipped with a Peltier (solid-state thermoelectrically cooled) detector using Cu Kα radiation ($\lambda = 1.5456$ Å). Scanning electron micrographs (SEM) were acquired using a JEOL JSM-T300 instrument operating at 20 kV. Samples were sputtered with gold to reduce charging. Thermogravimetric analyses (TGA) were carried out on a Perkin-Elmer Pyris 1 thermogravimetric analyzer with a heating rate of 20 °C/min and N_2 purge gas at a flow of 40 mL/min. Nitrogen adsorption and desorption isotherms were obtained on a Micromeritics ASAP 2010 instrument. Mesoporous silica was degassed overnight at 100 °C under vacuum prior to measurement; DNA-containing samples were degassed at 40 °C under vacuum overnight to avoid denaturing the material. Surface areas and pore size distributions were calculated using the BET and KJS[39] methods, respectively. Confocal fluorescence microscopy was performed on a Bio-Rad MRC-1000 instrument using an excitation wavelength of 488 nm. UV−visible spectra were recorded on a Perkin-Elmer Lambda 35 spectrophotometer. The solid-state ^{29}Si MAS NMR spectra were measured on a Bruker model ARX-500 spectrometer at a resonance frequency of 99.35 MHz. The powdered samples were placed in 7.0-mm-diameter zirconia rotors and spun at a rate of 4.0 kHz. A 30 s recycle delay was used between pulses. The chemical shifts were referenced to 3-(trimethylsilyl)-1-propanesulfonic acid sodium salt. Calcinations to remove surfactant prior to modification were carried out in a box furnace under conditions of flowing air. The following heating profile was used for calcinations: 2 °C/min ramp to 450 °C, 240 min hold at 450 °C, 10 °C/min ramp to 550 °C, 480 min hold at 550 °C.

Double-stranded calf thymus DNA, consisting of approximately 2000 base pairs, was purchased from Invitrogen and was used as supplied. As stated by the manufacturer, the DNA is double-stranded and consists of approximately 2000 base pairs. Fluorescein-labeled dUTP and PCR reaction components were purchased from Roche Molecular Biochemicals. Nucleotide primers for the gene for green fluorescent protein (GFP) were ordered from Invitrogen and diluted with TE buffer (10mM Tris-HCl, 1mM EDTA, pH 8.0). Tetraethyoxysilane (TEOS, 98%) and cetyltrimethylammonium bromide (CTAB) were obtained from Aldrich and used as received. Parr autoclaves were purchased from the Parr Instrument Corporation. All other chemicals were purchased from Sigma and used as received.

Synthesis of APMS. A solution of water (39.6 g), ethanol (100 wt %, 11.1 g, 232 mmol), and concentrated HCl (4.4 g, 12.2 M, 40 mmol) was prepared. CTAB (1.8 g, 4.9 mmol) was then dissolved in this solution, and NaF (4.76 g, 113 mmol) and TEOS (4.0 g, 19.2 mmol) were added simultaneously. The mixture was stirred until it became cloudy (∼90 s), at which point it was immediately transferred to a Teflon bottle and heated at 100 °C for 40 min. The resulting mixture was cooled to room temperature, filtered, washed, and calcined. The average pore diameter of APMS could be easily increased by a previously published method.[40] In a typical preparation, calcined APMS (3 g) was suspended in NH_4OH (75 mL, 1 M, 75 mmol) in a Teflon bottle, and the mixture was heated at 100 °C for various times; longer reaction times yielded larger pores and broader pore size distributions.

Surface modification of APMS materials was accomplished by reacting 500 mg dry APMS with 3-aminopropyltriethoxysilane (APTES, 0.92 g, 4.15 mmol) at reflux in toluene (20 mL) for 24 h. The resulting suspension was filtered, washed with toluene and methanol, and dried overnight under heat and vacuum to yield aminopropyl-modified APMS.

Incorporation of Metals into APMS. APMS was loaded with metals prior to DNA adsorption by stirring the calcined material for 30 min in 0.1 M solutions of $MgCl_2$, $CaCl_2$, or Na_3PO_4 buffer (50 mL solution/0.1 g APMS). The mixture was then filtered and the procedure repeated twice. The resulting metal-doped APMS was dried at 100 °C overnight.

Synthesis of Labeled Linear GFP-DNA. A solution of deionized H_2O (100 mL), LB Broth base (2.0 g), and ampicillin (1 mL of a 100 mg/L solution) was prepared in a 150 mL flask. It was then autoclaved, and after cooling it to room temperature, 100 μL of an ampicillin-resistant *E. coli* strain with a DNA plasmid containing the gene for green fluorescent protein (GFP) was added. The growth mixture was then incubated at 36 °C for 48 h. After this time, the culture was removed and refrigerated. The *E. coli* DNA was isolated and purified using a Wizard Plus Minipreps DNA Purification System (Promega). DNA replication and amplification of the GFP gene were achieved by the polymerase chain reaction (PCR) process. The base pair sequence of the forward primer (5′ to 3′) was AGC TGC TAT GTT GTG TGG; the sequence of the reverse primer (3′ to 5′) was GTG GTC TCT CTT TTC GTT GG.

Preparation of APMS−DNA Conjugates. Adsorption isotherms were obtained by preparing a series of DNA solutions with concentrations ranging from 1 to 200 μg/mL in either a 0.1 M solution of the appropriate metal ion or pure water (for surface-modified APMS). In each experiment, 1 mL of the DNA solution was applied to 10 mg of metal-exchanged APMS, and the resulting mixture was continuously shaken at 500 rpm at room temperature for 24 h. The mixtures were then centrifuged and filtered with 0.22 μm Millipore PVDF filters to ensure that

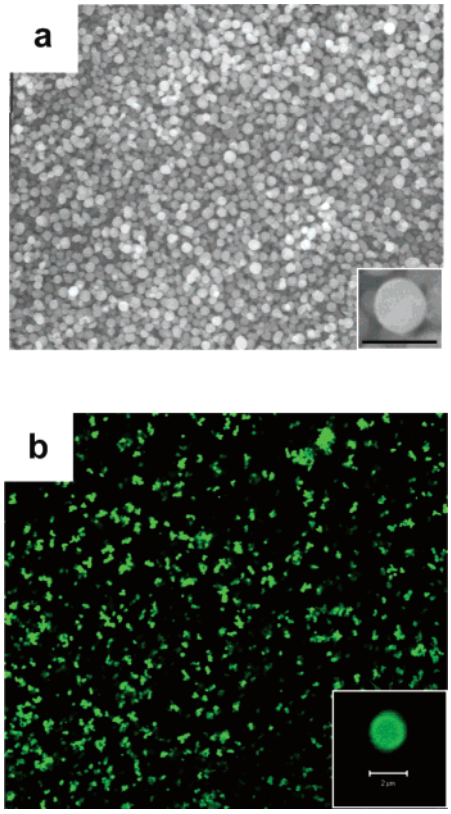

Figure 1. Microscopy of APMS-34: (a) SEM image of APMS-34 (bar = 3 μm) and (b) fluorescence CSLM image of APMS-34 after adsorption of double-stranded DNA labeled with fluorescein-488 (bar = 2 μm).

all silica particles were removed from the solution, which minimizes interference in subsequent spectrophotometric experiments due to light scattering of suspended APMS particles. The amount of DNA adsorbed by APMS was calculated from the difference in the concentration of DNA before and after addition of APMS, as determined by UV absorption at 260 nm. Triplicate samples were run for each experiment. Blank solutions were prepared by mixing 10 mg silica with each of the buffer solutions. Calibration experiments were carried out to account for any changes in adsorption caused by the presence of increased ionic conditions.

Results and Discussion

Although other studies have examined the attachment of DNA to the external surfaces of silica nanoparticles, the aim of this study was to examine DNA exchange into the pores of mesoporous silica. At room temperature, DNA adopts a helical geometry with an estimated cross-sectional diameter of approximately 19 Å, which should allow it to be incorporated into mesoporous silica (typical pore diameters 30−100 Å). In particular, APMS is a good candidate for biological applications, since it has a spherical shape that can easily be identified by microscopy and it is highly monodisperse (Figure 1a). In preliminary experiments to qualitatively confirm whether DNA can diffuse into the pores of APMS with 34 Å pores, linear DNA molecules of approximately 760 base pairs were fluorescently labeled during the PCR process by including a percentage of Fluorescein-488-labeled dUTP into the PCR mixture. The linear sequence chosen was that of the green fluorescent protein (GFP), since its sequence has been well-characterized. Linear DNA labeled in this manner was subsequently applied to APMS in a 0.1 M $MgCl_2$ solution for 24 h. The resulting conjugate

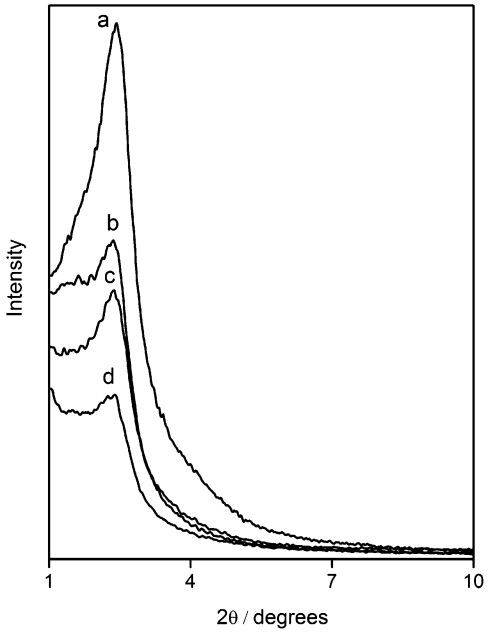

Figure 2. Powder XRD patterns of (a) unmodified APMS-34 and modified derivatives: (b) AP-APMS-34, (c) DNA-doped APMS-34, and (d) DNA-doped AP-APMS-34.

was studied with fluorescence confocal scanning laser microscopy (CSLM) at an excitation wavelength of 488 nm (Figure 1b). Since the CSLM technique allows optical sections of the particles to be taken, the presence of fluorescent molecules within the pores of APMS can be observed; a spherical image indicates that the DNA has penetrated throughout the interior of the particles, while a ring indicates that the DNA is located only on the outer surfaces. This image therefore indicates that the labeled DNA molecules are able to diffuse into the pores in short periods of time.

For experiments involving the characterization of APMS-DNA conjugates and more quantitative uptake studies, three materials were prepared, with pore diameters of 34, 54, and 100 Å, and were designated APMS-34, -54, and -100. The latter two materials were prepared by first preparing APMS-34 and then using previously published postsynthetic treatments to enlarge the pores of the material.[40] Since much more DNA was required than could be easily provided by PCR of the GFP gene, we chose to use a calf thymus DNA sequence of approximately 2000 base pairs for these studies.

Physical Characterization of APMS and DNA-loaded APMS. The XRD patterns of the APMS materials used in these studies are shown in Figure 2. The presence of only a single broad diffraction peak near 2.4° for the parent material, APMS-34 (curve a), is an indication of its amorphous nature.[32,34,41] The diffraction pattern of the related material, Mg^{2+}-APMS-34, after adsorption of DNA (curve c) shows a decrease in the intensity of the diffraction peak. This is indicative of the presence of a guest molecule inside the pores of the APMS and is attributed to the decreased density difference between the silica walls and the pore relative to the parent material.[42] The XRD pattern of aminopropyl-modified APMS-34 ("AP-APMS-34", curve b) decreases slightly in intensity due to the presence of the organic functionality. However, a much more significant reduction in intensity is seen after adsorption of DNA into the pores of this material (curve d), which indicates greater adsorption of DNA into the pores of the aminopropyl-modified material than in the presence of metal cations. Similar results were observed for APMS-54 and -100 and for materials containing Ca^{2+}.

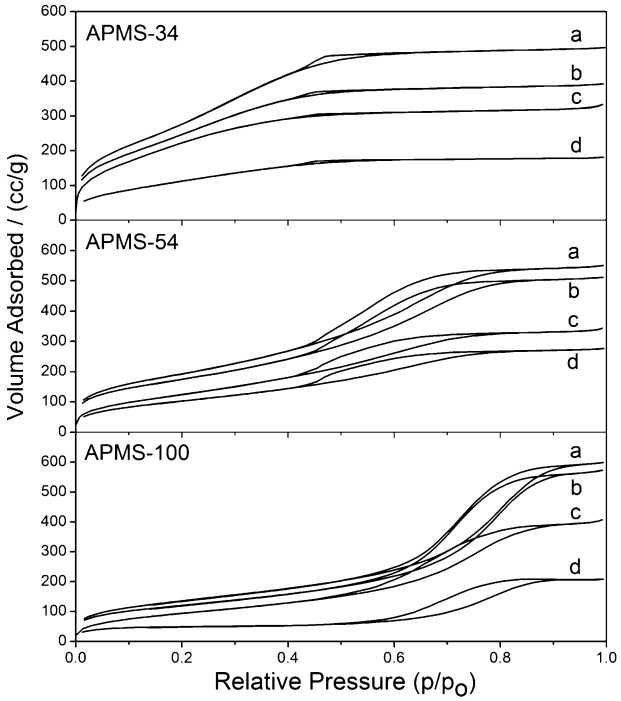

Figure 3. Nitrogen physisorption isotherms of APMS-34, -54, and -100 and their derivatives: (a) parent APMS, (b) DNA-doped Mg^{2+}-APMS, (c) AP-APMS, and (d) DNA-doped AP-APMS.

TABLE 1: Physical Data of APMS Materials

sample	surface area (m^2/g)	pore volume (cm^3/g)	pore size (nm)	AP linker (mmol/g silica)	AP linker (μmol/m^2)
APMS-34	971	0.91	3.4		
APMS-54	715	0.94	5.4		
APMS-100	500	1.0	10		
Na-APMS-54	670	0.97	5.7		
Ca-APMS-54	660	0.99	5.7		
Mg-APMS-54	631	0.99	5.7		
AP-APMS-34	854	0.71	2.8	2.2	2.6
AP-APMS-54	473	0.65	4.7	2.2	4.7
AP-APMS-100	357	0.73	8.4	2.2	6.2

The textural properties and corresponding nitrogen adsorption isotherms of APMS-34, AP-APMS-34, and DNA-doped APMS materials are shown in Table 1 and Figure 3. APMS-34 showed the large BET surface area (946 m^2/g) and pore volume (0.91 cm^3/g) that are characteristic of mesoporous materials. The average pore size distributions of APMS-34, -54, and -100 are shown in Figure 4, which indicates that the pore expansion process, which can be controlled simply by monitoring the time that the parent material spends in an ammonium hydroxide solution, is successful in increasing the average pore diameter. However, a consequence of the pore expansion is that the surface areas of APMS-54 and APMS-100 decreased to 715 m^2/g and 500 m^2/g, while the pore volume of the materials increased to 0.94 cm^3/g and 1.0 cm^3/g, respectively. Subsequent ion exchange with a 0.1 M solution of Mg^{2+} followed by contact with DNA reduced the overall surface area and pore volume of all materials (Figure 3, curves b) indicating that DNA adsorption within the pore had occurred. Doping of APMS-34 with DNA (Table 2) resulted in the smallest decrease in surface area (−2.6%) but produced the largest reduction in pore volume (−23%). Similar studies on the adsorption of enzymes into porous materials noted a similar trend when pores were too small to accommodate guest molecules and became blocked by molecules that were partially adsorbed into the mesopores.[43] In this case, N_2 molecules, which are small relative to the pore diameter, may still diffuse into

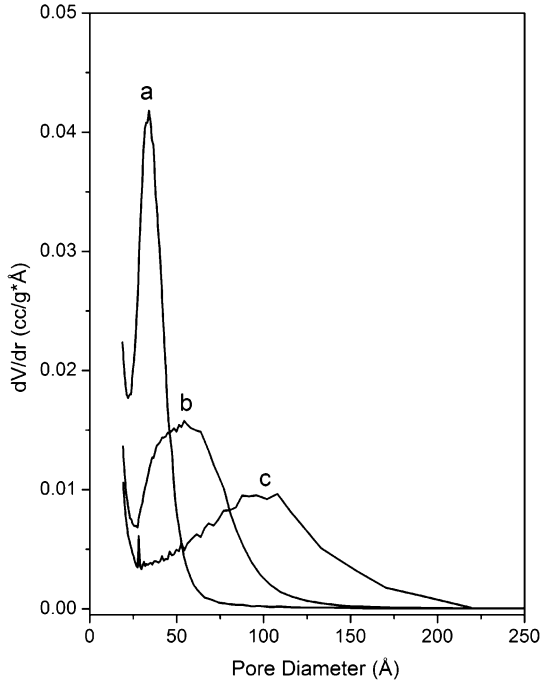

Figure 4. Average pore size distributions of (a) APMS-34, (b) APMS-54, and (c) APMS-100.

TABLE 2: Physical Data of DNA-doped APMS Materials

DNA doped sample	surface area (m^2)	Δ surface area (%)	pore volume (cm^3/g)	Δ pore volume (%)
Mg-APMS-34	946	−2.6	0.70	−23
Mg-APMS-54	641	−10	0.87	−7.9
Mg-APMS-100	440	−12	0.95	−4.9
AP-APMS-34	431	−50	0.33	−54
AP-APMS-54	389	−18	0.49	−25
AP-APMS-100	169	−53	0.34	−53

pores that are partially blocked by DNA molecules, accounting for the smaller decrease in surface area. The pore size of APMS-34 is large enough to accommodate the DNA molecule; however, the process is less favorable than for larger pore materials, since the DNA needs to be in an extended conformation to diffuse completely inside the pore. In contrast, some supercoiled DNA could fit into APMS-54 and APMS-100; this is confirmed by related studies involving size-exclusion chromatography of polystyrenes using APMS.[36] Accordingly, adsorption of DNA into the larger-pore APMS-54 and -100 materials resulted in a greater reduction in surface area with a smaller decrease in pore volume. This suggests that the DNA molecule is able to diffuse more completely into the larger-pore material. Modification of APMS with the organic linker resulted in a significant reduction in the surface area, pore volume, and average pore diameter of the base material, as shown by N_2 physisorption experiments (Figure 3, curve c). Subsequent exposure to DNA resulted in a much greater reduction of in total surface and pore volume compared to the magnesium doped materials (curves d); for example, the surface area of AP-APMS-100 was reduced by 53% from 357 to 169 m^2/g, indicating that adsorption of DNA into this material is quite favorable.

Effect of Metal Ion Identity and Concentration. Since it contains multiple phosphate sugar groups, at physiological conditions the entire DNA molecule behaves as a large, negatively charged polyelectrolyte. Ionic salts are known to promote DNA adsorption onto silica surfaces due to the mediation of the electrostatic repulsion between the negatively

TABLE 3: Calculated Langmuir and Freundlich Adsorption Constants and Linear Regression Values[a]

		Langmuir			Freundlich		
material	modification	b (μg/mg)	K_L (mL/μg)	R^2	A	K_F (mL^A μg^{1-A} mg^{-1})	R^2
APMS-34	Mg^{2+}	2.49	1.89	0.945	**0.707**	**0.20**	**0.982**
	AP	**9.26**	**0.39**	**0.995**	0.294	3.44	0.903
APMS-54	Na^+	0.22	0.27	0.330	0.163	0.10	0.645
	Ca^{2+}	2.17	0.09	0.980	**0.500**	**0.27**	**0.988**
	Mg^{2+}	**5.71**	**0.07**	**0.995**	0.697	0.40	0.885
	AP	**11.2**	**0.25**	**0.941**	0.395	3.02	0.550
APMS-100	Mg^{2+}	**4.25**	**0.07**	**0.985**	0.616	0.35	0.977
	AP	**15.7**	**1.46**	**0.940**	0.204	9.45	0.601

[a] The model that appeared to fit the data best is indicated in bold. This is the fit that is shown in the related figures.

charged silica surface and the DNA molecule.[44] The bridging behavior of the metal cation has been confirmed by Raman spectroscopy, which indicated that the metal binds to the phosphate backbone of the DNA molecule and not to the DNA bases.[45] Other groups have studied the differences in binding capacity of DNA to clay surfaces with various metal cations.[46−48]

For our studies, the adsorption of DNA into the pores of mesoporous materials was measured with respect to the equilibrium concentration of the DNA. Adsorption characteristics were studied using the common Langmuir[49] and Freundlich[50] models. The Langmuir model assumes monolayer adsorption onto homogeneous surfaces, whereas the semiempirical Freundlich model works well for heterogeneous surfaces at low concentrations that do not show a finite uptake capacity

$$C_e = K_L b C_s/(1 + K_L C_s) \qquad \text{(Langmuir)}$$

$$C_e = K_F C_s^{\,A} \qquad \text{(Freundlich)}$$

where C_e = the amount of DNA adsorbed onto the silica (μg/mg), C_s = the DNA concentration of the solution (μg/mL), b = the adsorption capacity of the solid (μg/mg), K_L = the Langmuir constant (mL/μg), and K_F (mL^A μg^{1-A} mg^{-1}) and A are empirical Freundlich constants. Calculated adsorption constants and the corresponding linear regression values are presented in Table 3. Consistent with studies of DNA adsorption onto clay surfaces, DNA adsorption into mesoporous materials was dependent on the identity of the metal cation present within the pores.[45,51] In a representative study, APMS-54 was used to generate DNA adsorption isotherms in 0.1 M salt solutions (Figure 5). DNA adsorption occurred quickly, with near-maximum adsorption completed within several minutes of application. The solid lines in this figure are drawn on the basis of the model that showed the best fit (either Langmuir or Freundlich). Maximum adsorption was seen to increase with the trend $Na^+ < Ca^{2+} < Mg^{2+}$. This trend is similar to that reported in studies on the adsorption of DNA onto other inorganic materials and confirms that divalent metals bind more strongly to DNA than monovalent ions.[46] In the absence of an ionic salt, no adsorption was observed; thus, it is clear that the ion is required for successful DNA adsorption. The Langmuir adsorption capacity of Mg^{2+}-APMS-54 was calculated to be 5.7 μg DNA/mg APMS, compared to 2.2 μg/mg for the Ca^{2+}-doped material. However, differences in the nature of the adsorption were observed for each cation. The Langmuir model fit well with the Mg^{2+} counterion while the R^2 regression values of both models fit well for the Ca^{2+} counterion. (In the latter case, the absence of any saturation limit at higher concentrations indicates that the Freundlich model better approximates its adsorption behavior, consistent with literature reports).[52] Negligible adsorption was measured in the presence of Na^+. These

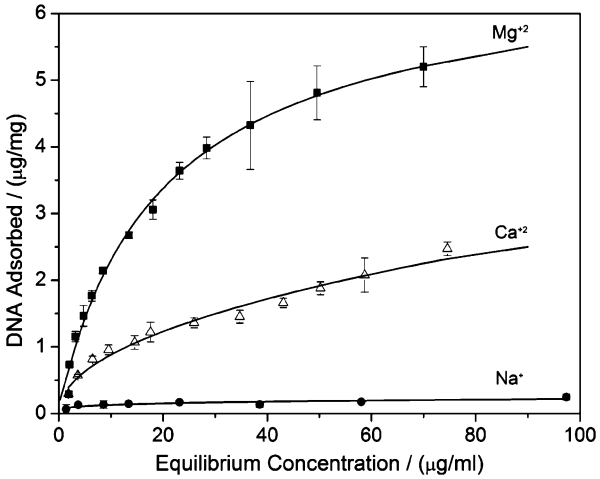

Figure 5. Comparison of DNA adsorption into APMS-54 doped with several metal cations. For Mg^{2+}, a Langmuir fit was used for the data; for Ca^{2+} and Na^+, a Freundlich fit was used.

variations suggest differences in the adsorption process. The Langmuir model assumes homogeneous and energetically equal binding sites, while the empirical Freundlich model is based upon multiple, energetically unique binding sites. The adsorption behavior at equivalent ionic strength suggests that Mg^{2+} is able to bind DNA more strongly than Ca^{2+}.

Effect of Pore Diameter. APMS materials with varying pore sizes were synthesized in order to study the effect of pore diameter on DNA adsorption. On the basis of the data obtained above with respect to counterion identity, Mg^{2+} was selected for adsorption studies related to the pore diameter of the silica substrate. The DNA adsorption isotherms of APMS materials with varying pore diameters are shown in Figure 6. APMS-34 adsorbs the least amount of DNA, while APMS-54 shows the highest maximum adsorption capacity at 5.7 μg/mg. Interestingly, APMS-100 adsorbs less DNA (4.3 μg/mg) than the 54 Å pore material, despite its larger pores. To further understand the adsorption behavior of these materials, DNA adsorption capacity was compared relative to the total surface area. Figure 7 presents the specific surface adsorption of the DNA. APMS-34 clearly adsorbs much less DNA per unit surface area than the other materials, indicating that pore diameter limitations are hindering the diffusion of DNA into the pore. However, APMS-54 and -100 have nearly identical specific adsorption capacities. This indicates that, as long as the DNA can enter the pores easily, surface area and presumably therefore the amount of loaded cation determines the loading capacity of the materials. Therefore, the smaller overall surface area of the 100 Å material accounts for its reduced DNA uptake.

In the experiments described in the previous section, the pore diameter remained the same, and therefore, the Langmuir and

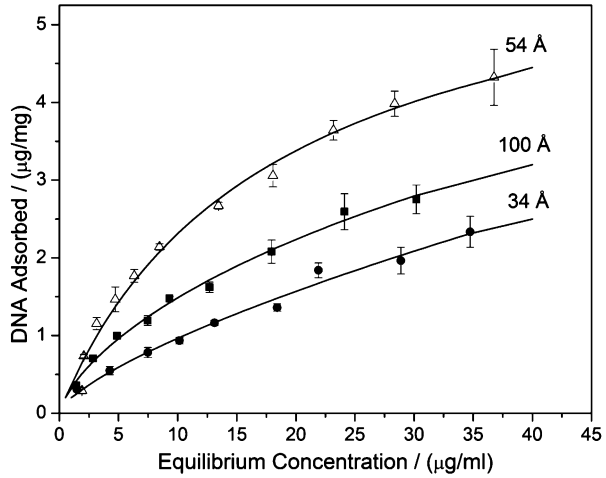

Figure 6. Comparison of DNA adsorption isotherms of Mg^{2+}-doped APMS with several pore diameters. A Langmuir fit was used for the 54 and 100 Å materials; for the 34 Å material, a Freundlich fit was used.

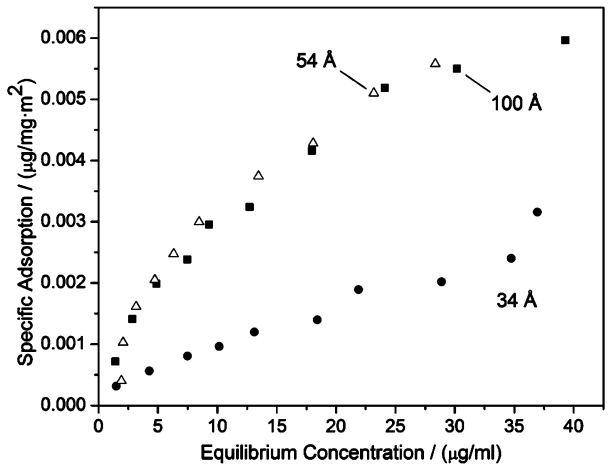

Figure 7. Comparison of specific DNA adsorption isotherms of Mg^{2+}-doped APMS with several pore diameters. Data in Figure 6 were normalized for the surface areas of each material.

Freundlich constants were more important in evaluating the strength of the DNA−ion interaction. However, in these experiments, the adsorption constants among the three materials can be used to determine the extent of intermolecular interactions among the DNA. This is significant here, because the pore diameter changes, while the type of metal ion remains the same. In this case, a good fit to the Langmuir model can be taken as an indication that the DNA is adsorbed easily with little intermolecular interaction, while a fit to the Freundlich model indicates the presence of stronger intermolecular interactions on energetically heterogeneous surfaces.[53] Analysis of the adsorption profiles with the two models reveals that both the 54 and 100 Å materials agree well with the Langmuir model. APMS-54 and -100 have the same calculated K_L value of 0.07 mL/mg. In contrast, APMS-34 fit poorly to the Langmuir model and is much better represented by a Freundlich isotherm. This suggests that intermolecular interactions between the DNA molecules are significant when the pore diameter is small, since the molecules compete for available adsorption sites and diffusion limitations in to and out of the pore are present. Accordingly, increasing the DNA concentration of the solution increases adsorption into the pores without a distinct saturation limit. This behavior is unique to APMS-34; apparently, the pores of the 54 Å materials are large enough that the adsorption behavior of DNA is altered.

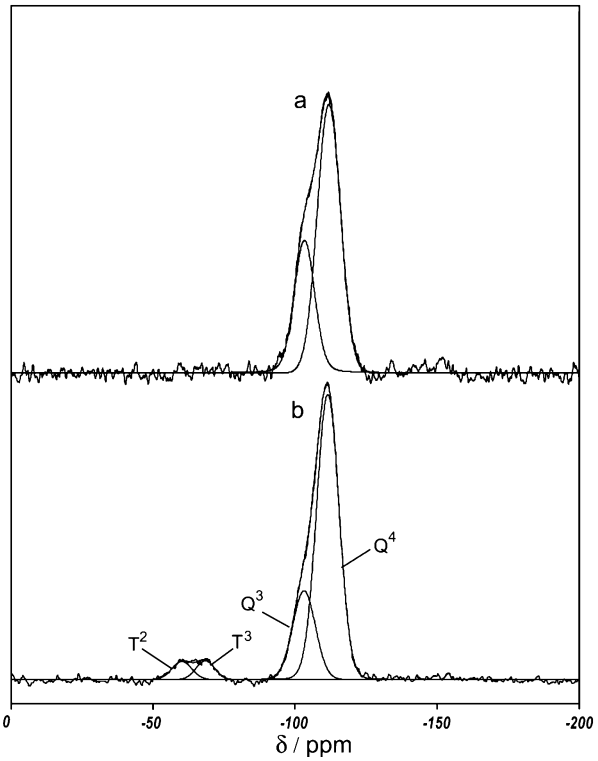

Figure 8. ^{29}Si MAS NMR of (a) APMS-34 and (b) AP-APMS-34.

Effect of Aminopropyl Linker. Our intention in studying aminopropyl-modified APMS was to compare surface-bound ammonium cations to exchangeable metal cations. Generally, silica surfaces are negatively charged and require charge mediation to bind DNA.[12,48,54] Covalently modifying silica surfaces to permanently locate a positive charge on the surface is expected to produce more efficient DNA binding compared to using an ionic salt solution, since the positive charge is covalently linked to the surface and should be constant regardless of solution composition. Other groups have attempted to graft cationic linkers to the outer surface of silica nanoparticles in order to increase the uptake of polyelectrolytes.[11,12,54,55] However, these studies did not attempt to quantitatively compare the increase in DNA uptake in materials containing linkers versus those without linkers. We used aminopropyl-modified APMS since it is easy to synthesize, and in aqueous solutions with pH values below the pK_a of the amino group ($pK_a = 9.64$), the surface of aminopropyl-modified APMS should have a net positive charge.[11,12]

Solid-state ^{29}Si MAS NMR was used to confirm modification of the silica surface with the silane linker. Figure 8 shows the spectra of the parent APMS-34 material (curve a) and AP-APMS-34 (curve b). The parent material is highly condensed, with a large fraction of the silica species in the fully condensed $Si(-OSi_4)$ state, as shown by the large Q^4 peak at −111 ppm ($Q^4/Q^3 = 2.2$). A small fraction of partially condensed $Si(-OSi)_3(-OH)$ (Q^3) species were also seen, as indicated by the appearance of a shoulder around −102 ppm. After modification, a decrease in the Q^3 shoulder is seen ($Q_4/Q_3 = 3.2$) along with a corresponding appearance of T^3 and T^2 [$Si(-OSi)_3(-R)$ and $Si(-OSi)_2(-OH)(-R)$] peaks, with shifts of −68 and −60 ppm, respectively, indicating that the aminopropyl linker was successfully attached to the parent APMS material.

Thermogravimetric analysis (TGA) revealed the extent of modification to be similar for all materials (∼2.2 mmol linker/g silica); however, after normalization to the surface area of each sample, APMS-100 had the highest extent of modification (6.2

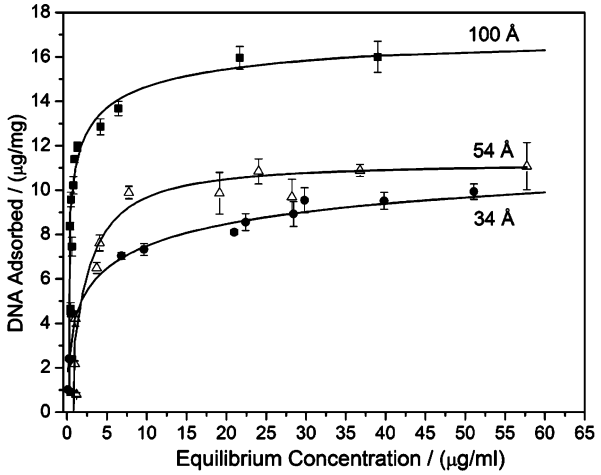

Figure 9. Comparison of DNA adsorption isotherms of aminopropyl-modified APMS with several pore diameters. The Langmuir model was applied to the data.

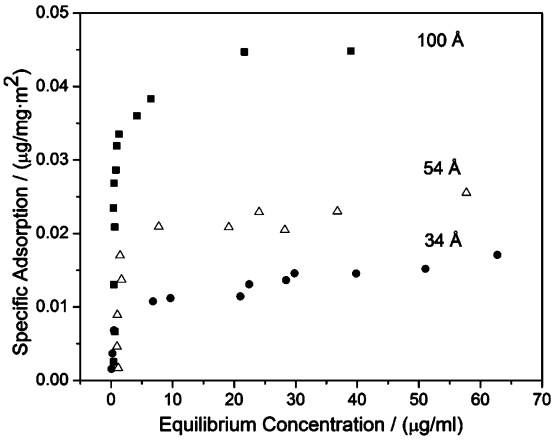

Figure 10. Comparison of specific DNA adsorption isotherms of aminopropyl-modified APMS with several pore diameters. Data from Figure 9 were normalized to the surface area of each material.

μmol/m^2). Figure 9 shows the adsorption of DNA onto AP-APMS-34, -54, and -100. Overall, DNA adsorption is markedly increased in comparison to APMS containing metal ions. For example, the maximum adsorption capacity of AP-APMS-100 was 15.7 μg/mg, compared to 4.3 μg/mg for Mg^{2+}-APMS-100. The difference in adsorption behavior and capacity between the metal cations and the aminopropyl linker could be explained by considering the differences between the two types of cations. First, the process of mediating the charge between the silica and the DNA using a metal cation would likely be entropically less favorable than the direct interaction of DNA with the aminopropyl groups that are covalently bound to the silica surface. This is because the former case involves a "trilayered" arrangement in which the metal cation interacts with both the anionic silica and the anionic DNA, while the latter case involves a direct electrostatic interaction between the cationic ammonium group and the DNA. Therefore, the equilibrium DNA adsorption is expected to be lower when metal cations are used. In addition, since metal cations are present in the solution used for DNA exchange, charge-neutralized DNA$-Mg^{2+}$ conjugates could also form in solution without adsorption to the silica surface. Overall, APMS-100 is able to bind more DNA per unit surface area than the other materials (Figure 10), in contrast to the results obtained for the metal-exchanged APMS. When comparing the calculated Langmuir constants, the 100 Å material has a much stronger affinity to bind DNA than the 54 Å material (K_L = 1.46 vs 0.25 mL/mg). The large pore material is therefore not only able to accommodate more DNA molecules per unit area, but also binds them more strongly. Additionally, as shown earlier, the postsynthetic modification of the silica with the aminopropyl linker decreases the effective pore diameter and pore volume of the material. Thus, APMS-54 begins to behave more like the smaller-pore APMS-34 material following modification with (aminopropyl)triethoxysilane.

Conclusions

Adsorption of DNA into APMS was studied by evaluating the relationships between cation identity and concentration, pore diameter, and surface area with respect to DNA adsorption. Confocal scanning laser microscopy revealed that fluorescently labeled DNA molecules were able to diffuse into the pores of APMS-34. XRD and N_2 physisorption studies before and after adsorption indicated that the DNA was located inside the pores and not exclusively on the external surface. DNA adsorption was found to be dependent on the type of metal cation used to mediate the charge between the DNA molecule and the silica surface, with DNA having a higher affinity for Mg^{2+} than either Ca^{2+} or Na^+. The diameter of the pore was also found to affect the amount of DNA that could be loaded into APMS. Materials with pores greater than 54 Å were found to be more favorable toward DNA adsorption, as the molecules could likely enter the pores without significant intermolecular interactions. Postsynthetic modification of APMS with APTES was found to dramatically increase DNA adsorption. AP-APMS with 100 Å pores adsorbed the largest quantity of DNA of any material studied. N_2 physisorption data indicated that DNA is better able to fill the pores of materials modified with APTES than metal cation-exchanged materials. Presumably, this is because the metal ions are not exchanged to their full capacity within the porous material, in turn limiting DNA uptake. Although incomplete at this time, preliminary studies of DNA desorption show that more DNA is released from metal-exchanged APMS than from APTES-modified materials. This agrees with the findings in this paper that the APTES-modified materials bind DNA more strongly. Currently, studies on the adsorption of cyclic DNA (i.e., plasmids used for gene expression) rather than linear DNA are being undertaken, and future work will focus on building a complete vector system based on APMS, including surface labeling of APMS for specific cellular targeting and uptake of DNA.

References and Notes

(1) Verma, I. M.; Somia, N. *Nature (London)* **1997**, *389*, 239.
(2) Hunt, K. K.; Vorburger, S. A. *Science* **2002**, *297*, 415.
(3) Marshall, E. *Science* **2001**, *294*, 1640.
(4) Miller, A. D. *Angew. Chem., Int. Ed.* **1998**, *37*, 1768.
(5) Kumar, M. N. V. R.; Bakowsky, U.; Lehr, C. M. *Biomaterials* **2004**, *25*, 1771.
(6) Oupicky, D.; Parker, A. L.; Seymour, L. W. *J. Am. Chem. Soc.* **2002**, *124*, 8.
(7) Kircheis, R.; Wightman, L.; Wagner, E. *Adv. Drug Delivery Rev.* **2001**, *53*, 341.
(8) Greenwald, R. B.; Choe, Y. H.; McGuire, J.; Conover, C. D. *Adv. Drug Delivery Rev.* **2003**, *55*, 217.
(9) Yamada, T.; Iwasaki, Y.; Tada, H.; Iwabuki, H.; Chuah, M. K.; Van den Driessche, T.; Fukuda, H.; Kondo, A.; Ueda, U.; Seno, M. *Nat. Biotechnol.* **2003**, *21*, 885.
(10) Choy, J.-H.; Kwak, S.-Y.; Jeong, Y.-J.; Park, J.-S. *Angew. Chem., Int. Ed.* **2000**, *39*, 4041.
(11) Csoger, Z.; Nacken, M.; Sameti, M.; Lehr, C. M.; Schmidt, H. *Mater. Sci. Eng., C* **2003**, *23*, 93.
(12) He, X.-X.; Wang, K.; Tan, W.; Liu, B.; Lin, X.; He, C.; Li, D.; Huang, S.; Li, J. *J. Am. Chem. Soc.* **2003**, *125*, 7168.
(13) Kneuer, C.; Sameti, M.; Bakowsky, U.; Schiestel, T.; Schirra, H.; Schmidt, H.; Lehr, C.-M. *Bioconjugate Chem.* **2000**, *11*, 926.

(14) Beck, J. S.; Vartuli, J. C.; Roth, W. J.; Leonowicz, M. E.; Kresge, C. T.; Schmitt, K. D.; Chu, C. T. W.; Olson, D. H.; Sheppard, E. W. *J. Am. Chem. Soc.* **1992**, *114*, 10834.
(15) Corma, A. *Chem. Rev.* **1997**, *97*, 2373.
(16) Kurganov, A.; Unger, K.; Issaeva, T. *J. Chromatogr., A* **1996**, *753*, 1770.
(17) Kisler, J. M.; Dähler, A.; Stevens, G. W.; O'Connor, A. J. *Microporous Mesoporous Mater.* **2001**, *44*−*45*, 769.
(18) Deere, J.; Magner, E.; Wall, J. G.; Hodnett, B. K. *Chem. Commun.* **2001**, *5*, 465.
(19) Hartmann, M. *Chem. Mater.* **2005**, *17*, 4577.
(20) Yoshitake, H.; Yokoi, T.; Tatsumi, T. *Chem. Mater.* **2002**, *14*, 4603.
(21) Ravindra, R.; Zhao, S.; Gies, H.; Winter, R. *J. Am. Chem. Soc.* **2004**, *126*, 12224.
(22) Ernst, S.; Hartmann, M.; Munsch, S. *Stud. Surf. Sci. Catal.* **2001**, *135*, 4566.
(23) Jia, L.; Katiyara, A.; Pintoa, N. G.; Jaroniec, M.; Smirniotis, P. G. *Microporous Mesoporous Mater.* **2004**, *75*, 221.
(24) Vinu, A.; Murugesan, V.; Tangermann, O.; Hartmann, M. *Chem. Mater.* **2004**, *16*, 3056.
(25) He, J.; Li, X.; Evans, D. G.; Duan, X.; Li, C. *J. Mol. Catal., B: Enzym.* **2000**, *11*, 45.
(26) Takahashi, H.; Li, B.; Sasaki, T. Miyazaki, C.; Kajino, T.; Inagaki, S. *Chem. Mater.* **2000**, *12*, 3301.
(27) Gómez, J. M.; Deere, J.; Goradia, D.; Cooney, J.; Magner, E.; Hodnett, B. *Catal. Lett.* **2003**, *88*, 183.
(28) Munoz, B.; Ramila, A.; Perez-Pariente, J.; Diaz, I.; Vallet-Regi, M. *Chem. Mater.* **2003**, *15*, 500.
(29) Song, S.-W.; Hidajat, K.; Kawi, S. *Langmuir* **2005**, *21*, 9568.
(30) Vallet-Regi, M.; Ramila, A.; del Real, R. P.; Perez-Pariente, J. *Chem. Mater.* **2001**, *13*, 308.
(31) Gallis, K. W.; Landry, C. C. U.S. Patent 6,334,988, 2002.
(32) Gallis, K. W.; Araujo, J. T.; Duff, K. J.; Moore, J. G.; Landry, C. C. *Adv. Mater.* **1999**, *11*, 1452.
(33) Ringenbach, C. R.; Livingston, S. R.; Kumar, D.; Landry, C. C. *Chem. Mater.* **2005**, *17*, 22, 5580.
(34) Sorensen, A. C.; Fuller, B. L.; Eklund, A. G.; Landry, C. C. *Chem. Mater.* **2004**, *16*, 2157.
(35) Gallis, K. W. Ph.D. Thesis dissertation. University of Vermont, Burlington, 2001.
(36) Nassivera, T.; Eklund, A. G.; Landry, C. C. *J. Chromatogr., A* **2002**, *973*, 97.
(37) Sorensen, A. C.; Landry, C. C. *Catal. Lett.* **2005**, *100*, 135.
(38) Fujiwara, M.; Yamamoto, F.; Okamoto, K. S.; Nomura, R. *Anal. Chem.* **2005**, *77*, 8138.
(39) Kruk, M.; Jaroniec, M.; Sayari, A. *Langmuir* **1997**, *13*, 6267.
(40) Mou, C.-Y.; Lin, H.-P. *Pure Appl. Chem.* **2000**, *72*, 137.
(41) Nassivera, T.; Landry, C. C. U.S. Patent Application #20060118490, December, 2005.
(42) Marler, B.; Oberhagemann, U.; Vortmann, S.; Gies, H. *Microporous Mater.* **1996**, *6*, 375.
(43) Deere, J.; Magner, E.; Wall, J. G.; Hodnett, B. K. *J. Phys. Chem. B* **2002**, *106*, 7340.
(44) Tian, H.; Huhmer, A. F.; Landers, J. P. *Anal. Biochem.* **2000**, *283*, 175.
(45) Langlais, M.; Tajmir-Riahi, H. A.; Savoie, R. *Biopolymers* **1990**, *30*, 743.
(46) Romanowski, G.; Lorenz, M.; Wackernagel, W. *Appl. Environ. Microbiol.* **1991**, *57*, 1057.
(47) Demanèche, S.; Jocteur-Monrozier, L.; Quiquampoix, H.; Simonet, P. *Appl. Environ. Microbiol.* **2001**, *67*, 293.
(48) Poly, F.; Chenu, C.; Simonet, P.; Rouiller, J.; Jocteur-Monrozier, L. *Langmuir* **2000**, *16*, 1233.
(49) Langmuir, I. *J. Am. Chem. Soc.* **1918**, *40*, 1361.
(50) Freundlich, H. *Colloid and Capillary Chemistry*, English translation of 3rd German ed.; Methuen: London, 1926.
(51) Gani, S. A.; Mukherjee, D. C.; Chattoraj, D. K. *Langmuir* **1999**, *15*, 7130.
(52) Wang, C.-M.; Chung, T.-W.; Huang, C.-M.; Wu, H. *J. Chem. Eng. Data* **2005**, *50*, 811.
(53) Ruthven, D. M. *Principles of Adsorption and Adsorption Process*; John Wiley & Sons: New York, 1984.
(54) Kneuer, C.; Sameti, M.; Haltner, E. G.; Schiestel, T.; Schirra, H.; Schmidt, H.; Lehr, C. M. *Int. J. Pharm.* **2000**, *196*, 257.
(55) Radu, D. R.; Lai, C.-Y.; Jeftinija, K.; Rowe, E. W.; Jeftinija, S.; Lin, V. S.-Y. *J. Am. Chem. Soc.* **2004**, *126*, 13216.